

MCS Analysis of Westinghouse 3-loop PWR Multi-cycle Operation

Bamidele Ebiwonjumi^a, Hyunsuk Lee^a, Jiwon Choe^a, Deokjung Lee^{a*}, Ho Cheol Shin^b

^aDepartment of Nuclear Engineering, Ulsan National Institute of Science and Technology, 50 UNIST-gil, Eonyang-eup, Ulju-gun, Ulsan, 44919, Korea

^bKorea Hydro & Nuclear Power Co. Central Research Institute (KHNP-CRI), Daejeon, Korea

*Corresponding author: deokjung@unist.ac.kr

1. Introduction

The application of Monte Carlo (MC) method in reactor core analysis has attracted much interest over the years due to its advantages such as the ability to model arbitrary complex geometry with very few approximations, the use of continuous-energy cross-sections and its possibilities for high-fidelity physics simulation. In this paper, six cycles operation of a Westinghouse 3-loop (WH3L) pressurized water reactor (PWR) is modeled and simulated by the MC code MCS under development at the Ulsan National Institute of Science and Technology (UNIST). This modeling and simulation is conducted for the verification of MCS refueling capability and the capability of MCS to solve whole core depletion multi-cycle problems of PWR. For the WH3L, neutronics and thermal hydraulic (TH) parameters are analyzed and selected results of four cycles are presented.

2. Computational Models and Methods

2.1 Westinghouse 3-loop PWR

The WH3L PWR is operated at 2900 MWth. The loading patterns for three cycles are shown in Fig. 1. Cycle $n+5$ uses the same loading pattern as cycle $n+4$. There are 157 fuel assemblies (FAs) in the whole core with 17 x 17 array of fuel rods and 25 guide tubes. FA type of "RFA" and "ACE7" are loaded into the core. The burnable absorber is $\text{UO}_2\text{-Gd}_2\text{O}_3$ with gadolinia content of 6.05 – 8.11 w/o. Using the core symmetry for computational efficiency, a three-dimensional (3D) quarter core model of WH3L is developed for MCS. The active core is divided into 24 axial nodes. The gadolinium pins are divided into 10 radial rings to accurately model the strong spatial self-shielding and large absorption reaction rates. The UO_2 fuel pins are not subdivided radially (1 cylindrical radial mesh only). The core baffle, barrel and spacer grids along the axial length of the FA are modeled in detail.

2.2 Monte Carlo Code MCS

MCS is a 3D continuous-energy radiation-transport MC code under development at UNIST. MCS is designed for the analysis of large scale nuclear reactors. The verification and validation of MCS neutron

physics covers ~300 critical cases of the International Criticality Safety Benchmark Experimental Problem (ICSBEP) [1], BEAVRS benchmark [2], VENUS-2, and Hogenboom Martin benchmark [3].

The WH3L core depletion is conducted by MCS with TH feedback, equilibrium xenon, and critical boron concentration (CBC) search. Burnup calculations are performed by the Chebyshev Rational Approximation Method using 1367-nuclide chain and a semi predictor-corrector depletion scheme. Gadolinium pins are depleted by the quadratic depletion method [4]. On-the-fly processing capabilities of MCS are used to generate temperature-dependent cross sections. Multipole representation is used to calculate Doppler broadened cross-sections in the resolved resonance range. $S(\alpha, \beta)$ data is used to treat thermal scattering in a bound target nucleus. Doppler Broadening Rejection Correction is applied to account for resonance scattering due to thermal motion of heavy target nuclides. The probability table method which is used to account for the effect of self-shielding in the unresolved resonance range (URR) is turned off, and average cross-sections are used.

The TH feedback is based on a one-dimensional (1D) single-phase closed-channel model which receives the power distribution from MCS and updates the coolant density and temperature distributions of fuel and coolant. All the WH3L simulations employ 5 inactive cycles, 20 active cycles, 200 sub-cycles per cycle, and 10,000 neutron histories per sub-cycle. The simulation time for one full reactor cycle amounts to about 4 days on 36 processors of type "Intel Xeon CPU E5-2680 @ 2.4 GHz". The memory used is about 14 GB per processor. Each transport plus depletion step takes about 4 hours. The calculations are performed at hot full power and all rod out state (ARO). In the 3D quarter core, there are 47 FAs and 442,944 depletion cells. The number of burnup steps is 22. The depletion of boron concentration in the moderator/coolant is not modeled.

It should be noted that the MCS calculations began in cycle n . For the beginning of cycle n (BOC n), individual fresh FA are depleted in MCS up to their respective burnups at the end of cycle $n-1$ (EOC $n-1$). The number densities from those depleted FAs are then used as refueling material at BOC n according to the loading pattern of cycle n . Subsequently, the material information at EOC n is used as material compositions

of burned FAs for BOC $n+1$, and so on. The results for cycles n to $n+1$ are not presented in this paper.

3. Results and Discussions

The results obtained from the reactor core multi-cycle depletion are presented in Figs. 2 – 8. The critical boron concentration as a function of burnup for cycles $n+2$ to $n+5$ is shown in Fig. 2. The measured CBC is obtained from the plant operation data and is the reference. Measured data for cycle $n+5$ is only available up to the middle of cycle (MOC). The Nuclear design report (NDR) results are obtained from the two-step method code system (PHOENIX-P/ANC). The STREAM/RAST-K2.0 results are obtained from STREAM and RAST-K2.0, a two-step lattice/neutron transport and nodal code system developed at UNIST for light water reactor analysis [5]. When MCS CBC is compared to measured data, the maximum difference is within 70 ppm throughout cycles $n+2$ to $n+5$.

Fig. 3 shows the axial distribution of the core TH parameters: fuel temperature, moderator temperature and density of cycle $n+2$ at BOC as calculated by MCS and STREAM/RAST-K2.0. The TH parameter at each height has been radially integrated across the core.

Measured assembly-wise power is determined using in-core detector signals obtained from 50 assemblies. The reference assembly power distribution is then generated with the INCORE code. Comparison of MCS axially-integrated relative assembly power distribution to INCORE results at BOC, MOC and EOC is shown in Figs. 4 – 7. The RMS error is less than 2% and the maximum relative difference of the assembly power distribution is within 5%. Throughout cycles $n+2$ to $n+5$, the maximum statistical uncertainty at one standard deviation of the assembly power predicted by MCS is 2.5% and this occurs at EOC $n+3$. Large discrepancies in the assembly power occur in the core periphery where the power is relatively low. In general, the distribution of relative differences is not perfectly four-fold symmetric. In addition, the relative differences in Fig. 7, which corresponds to the results of cycle $n+5$ assembly power distribution, is observed to show some tilt.

MCS axially-integrated relative pin power and flux distribution in cycle $n+3$ are presented in Fig. 8 at BOC, MOC and EOC. The dark red regions correspond to regions of fresh fuel loaded into the core for cycle $n+3$. The radial distribution of pin power and flux is noted to become more uniform with increasing burnup due to the temperature feedback.

4. Conclusions

Preliminary results of MCS applied to a Westinghouse 3-loop PWR core multicycle operation are presented in this paper. To the best of the authors' knowledge, this is the first time that a MC code is used to perform whole-core depletion analysis of a commercial light water reactor for more than two cycles: six consecutive cycles are simulated and results for four cycles are presented. Comparison to plant data measurement shows that MCS CBC is within 70 ppm and the assembly-wise power distribution RMS error is less than 2%. The results obtained can be considered acceptable because certain assumptions are made during the simulations such as the use of constant power, which is different from the real power history of the reactor, and the complete withdrawal of all the control rods, which would have been used to control the core reactivity and power levels during operation. Overall, this work shows that MCS can be applied in the analysis of whole core multicycle depletion of PWRs.

Acknowledgements

This work was partially supported by the National Research Foundation of Korea (NRF) grant funded by the Korea government (MSIT). (No. NRF-2017M2B2A9A02049916). This research was partially supported by the project (L17S018000) by Korea Hydro & Nuclear Power Co. Ltd..

REFERENCES

- [1] Jang, J., Kim, W., Jeong, S., Jeong, E., Park, J., Lemaire, M., Lee, H., Jo, Y., Zhang, P., Lee, D., Validation of UNIST Monte Carlo code MCS for criticality safety analysis of PWR spent fuel pool and storage cask. *Annals of Nuclear Energy* Vol. 114, p. 495, 2018.
- [2] Lee, H., Kim, W., Zhang, P., et al., Preliminary Simulation Results of BEAVRS Three-dimensional Cycle 1 Whole core Depletion by UNIST Monte Carlo Code MCS. *Proceedings of the M&C2017 conference*, Jeju, Korea, April 16 – 20 (2017).
- [3] Lee, H., Kim, W., Zhang, P., et al., Development status of Monte Carlo code at UNIST. *Proceedings of the Korean Nuclear Society Spring Meeting*, Jeju Korea, May 11 – 13 (2016).
- [4] Lee, D., Rhodes, J., Smith, K., Quadratic depletion method for gadolinium isotopes in CASMO-5. *Nuclear Science Engineering*, Vol. 174, p. 79, 2013.
- [5] Choe, J., Choi, S., Park, M., et al., Validation of the UNIST STREAM/RAST-K Code System with OPR-1000 Multi-cycle Operation. *Proceedings of the RPHA17 Conference*, Chengdu, China, August 24 – 25, (2017).

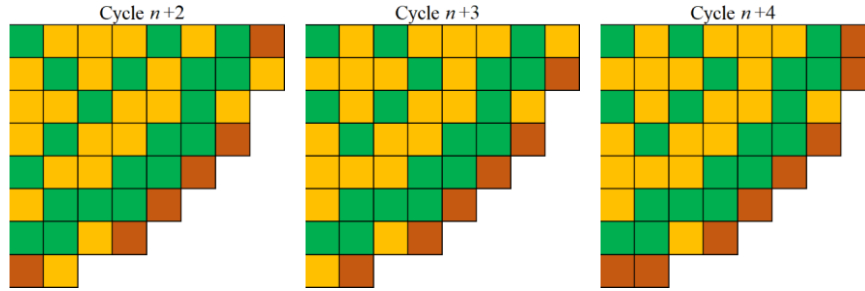


Fig. 1. Loading patterns of cycles $n+2$ to $n+4$. Legend: green (fresh FA), orange (once burned FA), brown (twice burned FA).

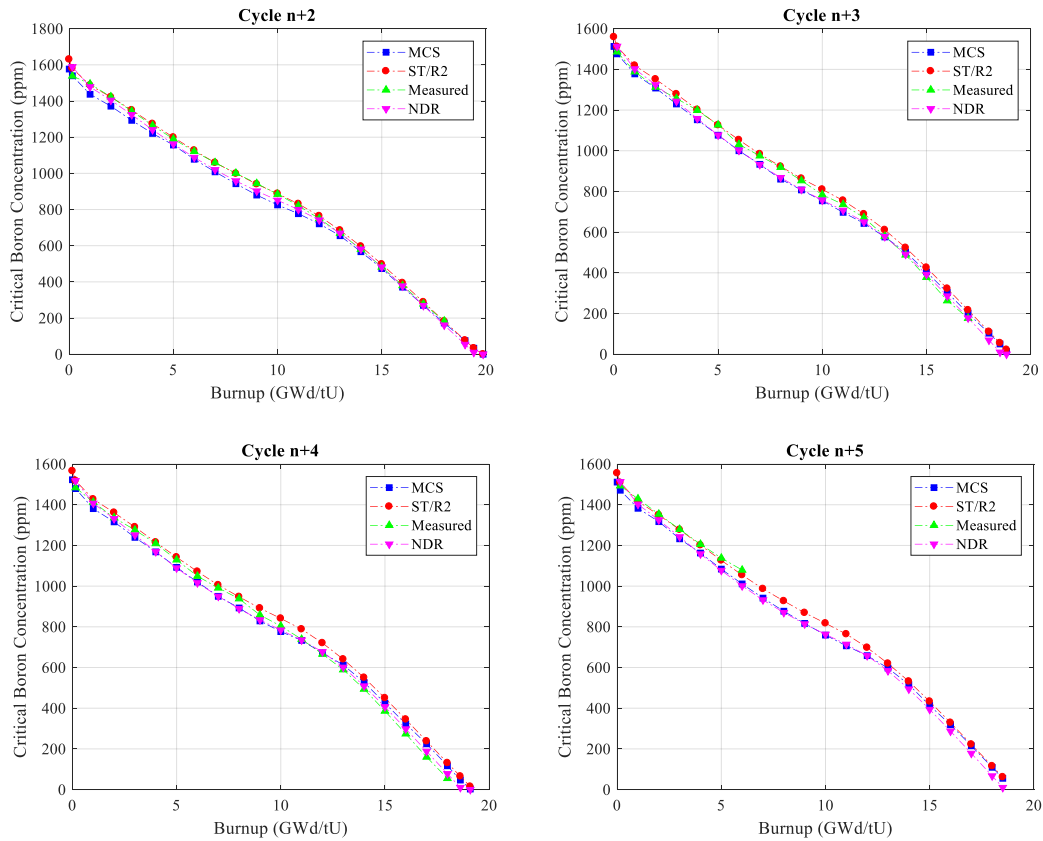


Fig. 2. Boron letdown curves of Cycles $n+2$ to $n+5$.

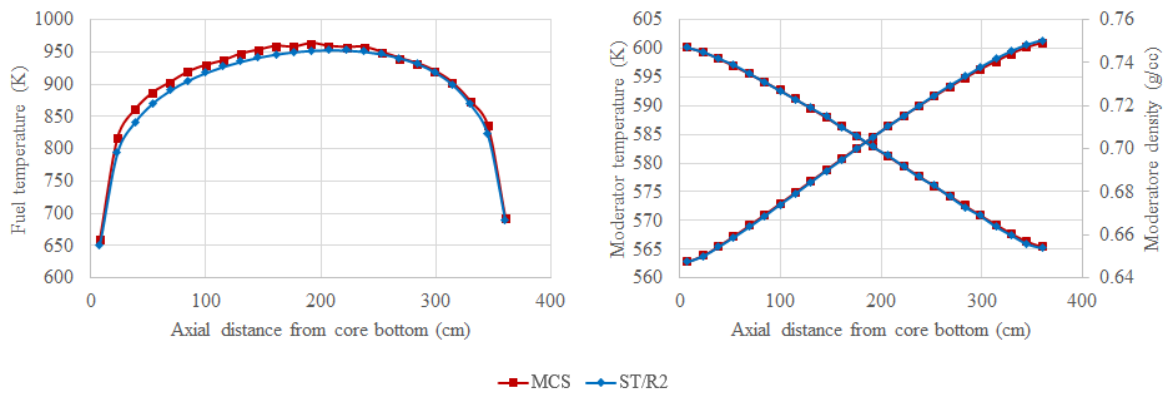


Fig. 3. Axial distribution of fuel temperature and moderator temperature/density of Cycle $n+2$ at BOC.

1.48	0.02	-0.13	-1.50	-0.62	0.60	-1.00	-4.14	-1.06	-1.31	-1.09	-0.46	0.77	1.35	1.06	-0.79	
0.07	-1.73	-0.90	-1.51	-0.35	-1.01	-0.71	-2.28	-1.20	-0.97	-1.11	-0.17	-0.16	1.16	1.39	0.67	
-1.39	-1.08	-1.15	-0.49	-0.81	-0.53	-0.79		-2.15	-1.71	-0.87	-0.86	-0.46	0.42	0.56		
-0.26	-1.46	-0.88	-1.10	-0.99	0.13	-0.37		-0.55	-0.64	-1.35	-1.20	-0.29	-0.19	0.27		
-0.65	-0.04	-0.78	-1.16	-1.29	-3.26			-0.08	-0.79	-0.49	-0.44	-0.10	-1.89			
0.30	-0.45	0.47	0.89	-4.05				0.11	0.80	0.39	-0.41	-2.46				
0.36	0.78	0.55	1.49					0.20	0.42	0.39	0.26					
-1.65	0.44							-2.42	-0.01							
							RMS								RMS	1.01
							Max								Max	2.46

Fig. 4. Relative differences (%) between MCS, INCORE assembly power of Cycle $n+2$ at BOC (left) and EOC (right).

0.66	-3.44	-2.64	-0.99	0.79	1.69	2.82	2.88	0.00	-1.61	0.90	-0.19	-0.71	-0.47	0.93	0.13	
1.82	-0.96	-1.77	-1.61	0.47	0.65	2.16	-0.49	0.77	-0.74	-0.04	0.97	-1.13	0.00	0.65	-0.81	
-1.96	-0.96	-2.52	-1.12	-0.02	0.78	1.35		0.29	-0.30	0.52	-0.11	0.00	0.42	0.43		
-0.22	-1.36	-1.70	-1.06	-0.89	1.36	0.63		-0.60	-0.02	-0.35	0.07	0.30	0.23	0.41		
0.88	0.19	-0.25	-1.33	-0.19	0.57			-0.92	-1.01	0.02	0.68	0.65	-0.74			
0.36	-0.07	0.83	1.12	0.02				-0.62	0.24	0.30	-0.25	-0.54				
2.29	2.26	0.87	0.45					0.38	0.34	-0.33	0.11					
3.26	0.06							0.36	-0.92							
							RMS								RMS	0.60
							Max								Max	1.61

Fig. 5. Relative differences (%) between MCS, INCORE assembly power of Cycle $n+3$ at BOC (left) and EOC (right).

0.33	0.20	-0.67	-0.29	-0.65	-2.04	0.73	0.77	-2.15	-1.86	-0.03	0.20	-0.67	-1.60	0.22	-1.62	
-0.45	-0.20	-0.27	-1.12	-0.58	-1.11	0.51	-2.66	-1.58	-1.59	-0.79	0.70	-0.45	0.27	0.05	-1.81	
-1.29	-0.67	-2.04	-0.87	-0.71	-0.68	-0.20		0.89	-0.28	0.01	-0.37	-0.06	0.16	-0.03		
0.05	-0.73	-1.41	-0.89	-1.04	0.24	-0.79		0.27	0.85	-0.79	-0.40	0.28	0.09	0.98		
2.39	1.76	-0.05	-1.22	-0.29	-1.48			0.74	0.52	0.24	0.08	0.23	1.00			
4.95	1.89	0.77	0.09	-1.61				2.21	1.60	0.83	0.21	-0.86				
3.94	3.14	1.73	-1.85					1.14	1.26	-0.08	0.04					
2.21	0.51							-0.07	-1.25							
							RMS								RMS	0.95
							Max								Max	2.21

Fig. 6. Relative differences (%) between MCS, INCORE assembly power of Cycle $n+4$ at BOC (left) and EOC (right).

2.18	2.66	1.62	1.34	-1.13	-1.58	-0.58	-4.54	0.80	0.63	0.38	1.20	0.35	0.29	0.16	-3.69	
2.02	2.24	2.01	0.55	-0.43	-2.12	-0.20	-2.34	0.20	0.01	0.22	0.76	0.70	-0.39	0.55	-1.37	
1.36	2.07	1.23	1.35	0.37	-1.43	-1.67		0.78	0.62	0.47	0.70	0.41	-0.01	-0.27		
2.02	1.26	1.72	0.12	-1.14	0.35	-3.23		1.15	1.42	1.23	-0.46	-0.92	0.26	-1.99		
-0.36	0.19	0.16	-1.35	-0.48	-1.49			-0.25	0.17	0.11	-1.15	-0.02	-1.34			
-1.45	-2.56	-1.38	0.40	-1.12				-0.90	-1.54	-1.09	-0.53	-1.73				
-0.86	-1.13	-1.67	-2.53					-0.06	-0.52	-1.18	-2.51					
-0.61	-2.99							1.85	-2.62							
							RMS								RMS	1.14
							Max								Max	3.69

Fig. 7. Relative differences (%) between MCS, INCORE assembly power of Cycle $n+5$ at BOC (left) and MOC (right).

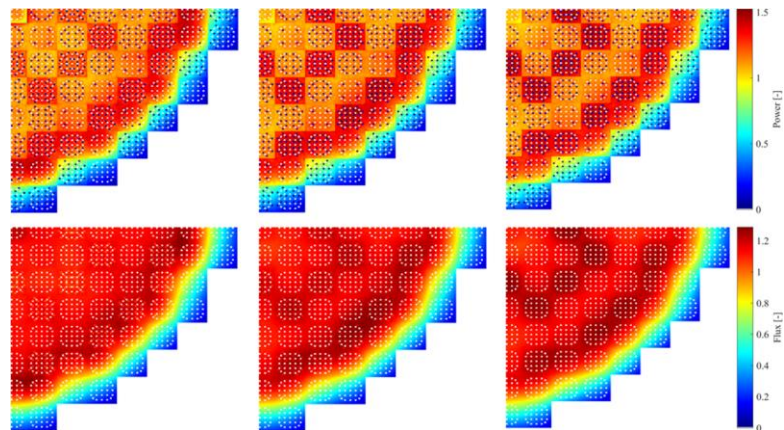


Fig. 8. MCS Cycle $n+3$ axially integrated radial pin power (top) and flux distribution (bottom) at BOC (left), MOC (center) and EOC (right).